2018

# Post-Translational Modification of Hypoxia-Inducible Factor Proteins by O-Linked -N-Acetylglucosamine in Breast Cancer Cells

Sean Williamson
*University of Mississippi. Sally McDonnell Barksdale Honors College*

# POST-TRANSLATIONAL MODIFICATION OF HYPOXIA-INDUCIBLE FACTOR PROTEINS BY *O*-LINKED β-*N*-ACETYLGLUCOSAMINE IN BREAST CANCER CELLS

by
Sean Edwin Williamson
with equal contribution from Hailey Grisham and Alexis Hill

A thesis submitted to the faculty of The University of Mississippi in partial fulfillment of the requirements of the Sally McDonnell Barksdale Honors College.

Oxford
May 2018

Approved by

_____
Advisor: Dr. Yu-Dong Zhou

_____
Co-Advisor: Dr. Dale George Nagle

_____
Reader: Dr. Kristopher T. Harrell

ACKNOWLEDGEMENTS

ABSTRACT
SEAN EDWIN WILLIAMSON: Post-Translational Modification of Hypoxia-Inducible Factor Proteins by *O*-Linked β-*N*-Acetylglucoseamine in Breast Cancer Cells

One of the hallmarks of cancer is its ability to adapt its metabolism to survive and thrive despite needing to overcome significant energy barriers and low oxygen settings in order to do so. The hypoxia-inducible factor proteins (HIFs) play important roles in the processes in which cancer fulfills these requirements. The *O*-linked β-*N*-acetylglucoseamine (*O*-GlcNAc) can be attached to cellular proteins through *O*-glycosylation, and is thus considered a potential target for anticancer mechanisms. HIFs are composed of α (HIF-1α and HIF-2α, respectively) and β subunits. This research found that *O*-GlcNAc is able to attach to and modify the HIFα proteins. This was accomplished through the use of immunoprecipitation followed by western blot, examining nuclear extract samples prepared from human breast cancer T47D cells. The *O*-GlcNAc was found to attach to both HIF-1α and HIF-2α, and was most prominently expressed in the presence of *O*-(2-Acetamido-2-deoxy-D-glucopyranosylidenamino) *N*-phenylcarbamate (PUGNAc), which enhances *O*-GlcNAcylation by inhibiting the enzyme OGA.

TABLE OF CONTENTS

LIST OF FIGURES

LIST OF TABLES

LIST OF ABBREVIATIONS

| | |
|---|---|
| βME | β-mercaptoethanol |
| BSA | bovine serum albumin |
| CE | cytoplasmic extract |
| CER | cytoplasmic extract reagent |
| DBPS | Dulbecco's phosphate buffered saline |
| dd | double distilled |
| DMEM/F12 | Dulbecco's Modified Eagle Medium/Nutrient Mixture F-12 |
| DMSO | dimethyl sulfoxide |
| ECL2 | enhanced chemiluminescence 2 |
| EDTA | ethylenediaminetetraacetic acid |
| FCS | fetal calf serum |
| HIF-1α | hypoxia-inducible factor-1 alpha |
| HIF-2α | hypoxia-inducible factor-2 alpha |
| HRP | horseradish peroxidase |
| LM | lung metastatic breast tumor cell line (LM4175) derived from triple-negative MDA-MB-231 human breast adenocarcinoma cells |
| MA | micro BCA reagent A |
| MB | micro BCA reagent B |
| MC | micro BCA reagent C |
| NE | nuclear extract |
| NER | nuclear extract reagent |
| *O*-GlcNAc | *O*-linked β-*N*-acetylglucoseamine |

| | |
|---|---|
| OGA | *O*-GlcNAcase |
| OGT | *O*-GlcNAc Transferase |
| PC-3 | human prostate adenocarcinoma cell line PC-3 |
| P/S | penicillin/streptomycin |
| PUGNAc | *O*-(2-acetamido-2-deoxy-D-glucopyranosylidenamino)-*N*-phenylcarbamate |
| T47D | human ductal carcinoma breast tumor cell line T47D |
| TBST | tris-buffered saline and tween 20 |

## Introduction/Background

Cancer represents a diverse set of diseases which involve the unusual, rampant growth of cells, which usually spread into neighboring tissues. The cellular cycle of life, replication, and death is interrupted, leading to cells surviving when they should be dying and often subsequently forming masses called tumors. These cancerous cells differ inherently from healthy cells in several ways which allow them to continue growing beyond their usual limits. Whereas healthy cells can obey cell-to-cell signaling, such as those signals that inform cells to stop growing so as to not cause damage, cancer cells ignore many of these chemical signals. Contrary to normal cells, cancer cells often do not mature into differentiated cells that specialize in their function. This can lead to repeated replication of immature cells, often picking up more genetic mistakes and variation, sometimes promoting further accelerated growth. These cancer cells are also unable to repair themselves as healthy cells can. Healthy cells may undergo apoptosis (programmed cell death) if they recognize permanent genetic damage, but cancerous cells often ignore the signals that initiate this process. Further, where healthy cells maintain their appropriate position to fulfill a physiological role in the body, cancer cells are often prone to detach and move throughout the body, a detrimental process which can lead to metastasis, wherein a mass attaches to a point in the body away from its origin and continues to grow. These cellular changes are initiated by multiple changes in one of two

types of genes; overexpression of cancer causing oncogenes or repression or disabling of tumor suppressor genes.

Along with this limitless replication, propensity to metastasize, resistance to apoptosis, and genome instability and mutation, there are six other universally accepted major characteristics of cancer[23]. One such characteristic is an ability to avoid growth suppressors. This can be accomplished through the disabling of tumor suppressor genes, but is also achieved by overcoming contact inhibition, which is a growth prevention method which shuts off division once cells are in contact with other cells on all sides[5]. Another hallmark of cancer is independence from external growth factors. This allows cancer cells to grow self-sufficiently, either by producing such signals themselves via autocrine signaling, by cutting negative feedback loops, or by permanently activating feed forward pathways to respond to its own autocrine signals[23]. Cancer cells also promote angiogenesis, or the formation of new blood vessels, in order to fuel a tumor's new need for blood and oxygen[5]. Along with genome instability, the last and most recent common characteristics of cancer include evasion of the immune system, deregulation of typical metabolism features and a subsequent elimination of cell energy limitations, and tumor caused inflammatory responses[5].

Cancers are classified by the cells from which they are derived. Thus, breast cancer develops from breast tissues and the tumor cells consequently resemble breast tissue cells. Diagnosis involves an initial breast examination screening by mammography followed by a biopsy, including analysis for estrogen and progesterone receptors and the human epidermal growth hormone receptor 2 (HER2) protein[9]. Symptoms of breast

cancer include lumps in the breast, changes in breast shape, fluid or blood excretions from the nipple, changes in skin texture or dimpling. Though only 0.1% of men will develop breast cancer throughout their lifetimes, an estimated one in eight women in the U.S. will develop the disease[21]. Breast cancer progresses through four stages, which increase in severity and are determined by taking into account the size of the tumor, whether it has spread to the lymph nodes, and whether the tumor has metastasized. Stage 0 is precancerous, stages 1 through 3 refer to tumors in the breast and lymph nodes, and stage 4 is metastatic and features the least optimistic prognosis. Stage 4 breast cancer cells may migrate to nearly any organ, but most commonly settle in bone, brain, liver, lungs, or skin tissue[9]. At stage 4, the five-year survival rate is around 22 percent. At stage 3 this rate is 72 percent and at stage 2 it is greater than 90 percent[14]. Thus, early detection and treatment is imperative. While all breast cancers originate in the breast tissue, there can be many variations of the disease. They vary in specific location, as tumors can form in either ducts, which are tubular passageways in the body through which secretions can flow, or lobules, which is glandular tissue throughout the breast that produces milk and leads into ducts. Breast cancers are also defined by invasiveness, or whether or not they spread to surrounding tissues. The most common breast cancers are ductal carcinoma in situ (DCIS), invasive ductal carcinoma (IDC), and invasive lobular carcinoma (ILC)[20]. Ductal carcinoma in situ is either non-invasive or pre-invasive and Stage 0, whereas both IDC and ILC are invasive and pose risk of metastasis[20]. Other less common types of breast cancers include sarcomas, Paget disease, angiosarcomas, or inflammatory breast cancer.

The tumor microenvironment (TME) of a cancerous mass of cells encompasses the interaction between the tumor and the surrounding tissues, including the blood vessels, immune cells, fibroblasts, bone marrow-derived inflammatory cells, lymphocytes, signaling molecules, and extracellular matrix. The tumor microenvironment consists of immune system cells, tumor vasculature and lymphatics, fibroblasts, pericytes, and the malignant cancer cells[1]. This TME affects how the tumor grows and evolves, while the tumor can affect the TME by releasing extracellular signaling molecules, promoting angiogenesis (new blood vessel formation), and causing immune tolerance and inflammation[8]. One key example of the interaction between the tumor and its environment is the formation of vasculature. Angiogenesis is controlled by over a dozen angiogenic activator and inhibitor proteins, the levels of which reflect the aggressiveness of the cancer[15]. Cancer cells must interact with nearby existing vasculature in the TME using these proteins to form new vasculature to enable tumor growth and survival. The tumor microenvironment and its associated growth and maintenance is heavily dependent on this newly formed vasculature, as it, like healthy tissue, requires both blood and lymphatic networks to provide oxygen and remove waste products. Once angiogenesis starts, there is continued development of new blood vessels, which are usually leaky and inefficiently perfused compared to healthy natural vasculature. This incomplete vasculature suppresses immune surveillance for the tumor cells, helping the cancer to largely evade host immune responses[23].

Another example of the interaction of tumors with the TME is in their response to inflammation. Inflammatory cells are a large part of the TME, and it has been found that inflammation is critical for tumor progression[6]. The surrounding fibroblasts, extracellular

matrix, and immune cells respond in a way similar to how they would counter a wound; aiding angiogenesis, preventing apoptosis, and speeding up the cell cycle. All of this encourages tumorigenesis[10]. Inflammation is the result of a network of signals initiated at the time of tissue injury in order to heal wounds. Tumor cells are capable of producing cytokines and chemokines, both of which can attract leukocytes and consequently initiate an inflammatory response. Cytokines are proteins that mediate communication between cells. They are synthesized by fibroblasts and endothelial cells in response to inflammation. They regulate cell differentiation, migration, death, and survival. Cytokines can produce an antitumor response, but also can promote cell transformation and malignancy in response to chronic inflammation[11]. Also involved with the TME, carcinoma associate fibroblasts (CAFs) are a group of fibroblasts which are taken over by cancer cells in order to promote angiogenesis by producing proangiogenic signaling proteins, including some which promote angiogenesis in tumors that are resistant to other angiogenesis promoting protein factors[6,23]. This contrasts with the healthy fibroblasts, which are typically anti-tumorigenic. The CAFs are also able to secrete transforming growth factor-beta (TGF-β), which promotes metastasis[16].

Tumor hypoxia is a critical element of the tumor microenvironment, and carries with it major implications for cancer cells. It occurs when tumor cells are deprived of oxygen. As tumors grow, they outgrow the existing vasculature, resulting in a lower oxygen concentration than other tissues of the same type. Causes of tumor hypoxia include an increase in the distance oxygen must diffuse between the tumor cells and the blood vessels, reduced oxygen transport capabilities of the blood due to anemia (caused by either the disease or treatment), and abnormalities in the structure and function of the

new tumor vasculature[22]. This lack of oxygen can act as a suppressor of the tumor by slowing proliferation or possibly even causing cell death. However, it can also result in increased progression and proliferation along with heightened resistance to cancer treatment through changes in the genome and proteins in the TME caused by the hypoxic conditions[22].

Hypoxia increases the already-unpredictable genomic instability of tumors, causing even more genetic mutations in cancer cells. This can result in the production of cells with greater survivability under hypoxic conditions which clonally expand and propagate a cycle of tumor cells with increasing survivability. The results of this selection can include tumor proliferation, metastasis, and resistance to radiation and chemotherapy. Correspondingly, hypoxic stress can cause changes in gene expression and the tumor cell proteome. These changes may be beneficial, as they have the potential to slow or stop growth by produce cell-cycle arrest at the $G_1$/S checkpoint as caused by activation of the cyclin-dependent kinase inhibitors p21 and p27 by hypoxia-inducible factor-1 (HIF-1). Hypoxia has also been found to cause p53 level to rise, possibly resulting in apoptosis, cause terminal differentiation of cells, and lead to necrotic cell death. While all these results can be considered beneficial to the overall health of the cancer patient, there can also be severely detrimental proteomic affects, as well. Cells may adapt to the hypoxic condition, or attempt to leave the hypoxic environment by local invasion or metastatic spread.  hif

Hypoxia-inducible factors (HIFs) are the body's natural transcriptional response to lowering oxygen concentration levels. When low cellular levels of usable oxygen are

detected, HIF transcription factors are upregulated. These transcription factors affect gene expression involved with alteration of metabolism, contributions to angiogenesis, remodeling of the extracellular matrix, metastasis, invasion, motility, cancer stem cell maintenance, evasion of immune system, and resistance to chemotherapy and radiation therapy[18]. Encoded for by the *HIF1A* gene, HIF-1α protein is the hypoxia-responsive subunit of heterodimeric transcription factor HIF-1. Hypoxia-inducible factor-1 induces transcription of over sixty genes, including those encoding proteins such as erythropoietin and vascular endothelial growth factor (VEGF)[22]. In response to varying oxygen levels, HIF-1 undergoes conformational changes and alters its transcriptional activity. This HIF-1α transcriptional activity is particularly sensitive to altered oxygen levels. Under conditions of normal oxygen levels, HIF-1α is rapidly ubiquitinated and degraded. Contrarily, under hypoxic conditions, this protein degradation is inhibited and HIF-1α accumulates. This HIF-1α subunit forms a heterodimer with a HIF-1β subunit, which instigate transcriptional activity on their target genes.

Overexpression of HIF-1 subunits HIF-1α and HIF-2α are correlated with increased tumor growth and metastasis due to their role(s) in creating new blood vessels and altering cell metabolism in order to counter hypoxia[12]. Apoptosis is a normal response to hypoxia; however, HIF-1 acts to prevent apoptosis in cancer cells in which it is overexpressed. Expression of HIF-1 has been found to be elevated in a number of cancers, including colon, breast, pancreas, kidneys, bladder, brain, ovary, and prostate[19]. In many of these and other cancers, overexpression of HIF-1 leads to heightened tumor progression and has been found to be indicative of resistance to certain treatments including radiation and chemotheraphy[18]. Overexpression of HIF-1α has been found in

the early pre-invasive stages of breast cancer and may even regulate the subsequent progression of breast tumors[3]. Overexpression of HIF-1α was also shown to be a predictor of poor cancer treatment response. Similar trends have also been observed in brain and ovarian cancers, as well as in breast cancers[2].

Due to the relative lack of oxygen and the increased proliferation that is exhibited in cancer cells, energy needs in tumors are higher than they are in healthy cells and it is more difficult for tumor cells to meet these increased energy demand by traditional means. Though tumor metabolism varies, one primary conserved factor of the metabolic changes associated with tumorigenesis is an overall improvement of cellular fitness that provides a selective advantage during tumor growth. This is commonly achieved through changes that aid cell survival during stress (such as hypoxia) or by changes that facilitate growth in times when cell growth should be otherwise suppressed. The Warburg effect is one such notable deviation from the norm for cancer cells. While healthy cells create energy most efficiently through utilization of mitochondria in oxidative phosphorylation, cancer cells typically create energy through glycolysis and lactic acid fermentation, even in the presence of oxygen. This process is aerobic glycolysis, or the Warburg effect, and is instigated by hypoxic conditions within the TME. Transcriptional activation of HIF-1 also induces alterations in tumor cell metabolism, such as increasing glycolytic variability. Other variations in metabolism used to counteract a hypoxic environment in cancer cells include using glutamine as a substrate for oxidative ATP production or by providing acetyl-CoA in order to promote cell proliferation[4].

Along with energy production, it is also immensely important for cancer cells to synthesize lipids and macromolecules, as this enables proliferation and growth of the tumors. Fatty acid synthesis produces important molecules that play important roles in tumor cell signaling and membrane biosynthesis. Acetyl-CoA is a necessary prerequisite for fatty acid production. In healthy cells, Acetyl-CoA is normally produced by the breakdown of glucose; however, in hypoxic or nutrient devoid environments, glutamine, acetate, and (in some cell lines) leucine are able to be utilized as carbon sources. Hypoxic conditions also suppress de novo fatty acid synthesis from glucose. Fatty acids may also be obtained for membrane biosynthesis from the extracellular space. In such cases, PI3K signaling initiates fatty acid uptake and prevents its degradation. This process can be regulated depending on the stress of the surrounding environment of the cell, and it is necessary for the most pronounced growth associated with hypoxic tumors[4].

The monosaccharide derivative of glucose, *N*-Acetylglucosamine (GlcNAc), has the molecular formula of $C_8H_{15}NO_6$. It is a part of both bacterial cell walls (peptidoglycan) and in the cell walls of fungi, and forms the polymer chitin in the outer shells of insects and crustaceans. The intracellular carbohydrate *O*-linked β-*N*-acetylglucosamine (O-GlcNAc) is found in the nucleus and cytoplasm which alters proteins on the serine and threonine hydroxyl groups. Protein modification by O-GlcNAc is especially relevant in many human diseases, one of which being cancer[7]. The process of O-GlcNAcylation is the covalent attachment of β-D-*N*-acetylglucosamine to serine or threonine residues and is important as a regulator in many cellular processes. It is associated with sensing capabilities, as O-GlcNAcylation rises in response to increased glucose and glutamine. As tumors are able to change their cell metabolism from oxidative

phosphorylation to the glycolytic pathway via the Warburg effect, glucose uptake is heavily increased. Meanwhile, cancer cells also increase glutamine uptake. The combination of these factors leads to an increase in O-GlcNAcylation and the continual transformation of the cancer cell metabolism in general[13]. The process of O-GlcNAcylation has been found to have a hand in cell signaling, transcription, replication, and cell metabolism, all of which can have cancer-related implications. It is catalyzed by *O*-linked *N*-acetylglucosamine transferase (OGT), an enzyme which transfers the *N*-acetylglucosamine from uridine diphosphate *N*-acetylglucosamine (UDP-GlcNAc) to a protein[7]. The process of *O*-GlcNAcylation has been found to be increased in a number of breast cancer cell lines and heightened OGT protein expression is attributed to more aggressive breast cancer cell lines[7].

## Methods and Materials

### Cell Culture/Compound Treatment

Human breast tumor T47D cells (ATCC) were maintained in RPMI160 medium (Corning) in the presence of fetal bovine serum (FCS, 10% v/v, Hyclone) and penicillin/streptomycin. Prior to compound treatment, T47D cells were detached from plates by trypsin and used to make seed plates for later use in SDS-PAGE and Western Blotting after later nuclear extractions and cytoplasmic extractions. The cells were grown overnight on a single 10 cm plate. Conditioned media was aspirated from this plate, and the plate was washed once with cold Dulbecco's Phosphate Buffered Saline (DBPS), diluted from 10x to 1x (Sigma Aldrich D1408). The cells were subsequently detached from the plate using approximately 0.9 mL of a 0.25% trypsin ethylenediaminetetraacetic acid (trypsin-EDTA) solution (Gibco 25200-056). The trypsin-EDTA solution was added at 37°C for five minutes. The addition of the trypsin to the 10cm cell plate effectively caused the white cells to detach from the media, and they slid slowly around the bottom of the plate. They clumped together after detaching, and flowed with the pink trypsin. 7.5 mL Dulbecco's Modified Eagle Medium/Nutrient Mixture F-12 (DMEM/F12) with 10% Fetal Calf Serum (FCS) was added, followed by penicillin/streptomycin (P/S) antibiotics. The resulting solution was pipetted thoroughly multiple times to mix. The cells were counted using a hemocytometer and an inverted microscope. A drop of the cell solution was added into the hemocytometer, which was pulled into the viewing area by capillary action. The hemocytometer was then viewed under the inverted microscope. Cells within

a 4x4 square grid on the hemocytometer were counted manually, with this process beingrepeated three other times for the other 4x4 square grids. These values were averaged, and that total multiplied by 10,000 in order to arrive at the approximate cell count per mL. The average cell count with the hemocytometer was 75 cells in the four by four grid, which, when multiplied by 10,000, indicated $7.5x10^5$ cells/mL. Cell-containing solution (10 mL) were with 5 mL of media to bring the final concentration to $0.5 \times 10^6$ cells/mL, which was used to create seed plates. Four small, 6 cm plates were seeded. $1.5 \times 10^6$ cells were used to seed each plate in a final volume of 3 mL which contained the cells and DMEM/F12. A larger seed plate was created using 1 mL $0.5 \times 10^6$ cells/mL with 9 mL DMEM/F12 media. The cells and media were mixed using a pipette, then incubated at 37°C overnight.

The plates were washed once with 3 mL cold DPBS diluted from 10x to 1x. Each of the four seed plates had a different compound added to them alongside 5% FCS with P/S. Three mL of 5% media was added to the first plate. Three µL of 10 mM 1,10-phenanthroline was combined with 3 mL dimethyl sulfoxide (DMSO), bringing the concentration of 1,10-phenanthroline to 10 µM, was added to the second plate. 0.9 µL of *O*-(2-acetamido-2-deoxy-D-glucopyranosylidenamino) *N*-phenylcarbamate (PUGNAc) at 100 mM concentration, bringing the concentration to 30 µM, was combined with 3 mL of DMSO and added to the third plate. The fourth plate contained 10 µM 1,10-phenanthroline and 30 µM PUGNAc. These four plates were incubated for four hours at 37°C.

**Nuclear/Cytoplasmic Extracts**

Nuclear and cytoplasmic extractions were performed on the T47D cells from these four seed plates. The media was first removed after the incubation, then approximately 2 mL DPBS was used to wash the cells. The DPBS was aspirated after washing. 300 µL trypsin was added and moved around the plates to detach the cells, followed by five minutes of incubation at 37°C. Media (1 mL) was added to each of the four plates, then the trypsin/media solution was mixed thoroughly over the cells with a pipette. The cells alongside the trypsin/media solution were transferred from each plate to a separate 2 mL centrifuge tube. Then, DMEM media (0.5 mL) was used to wash each plate again, then was again transferred from each plate to their respective 2 mL centrifuge tube. These tubes were counterbalanced and centrifuged in a microfuge at 850 rpm for four minutes.

The centrifuge tubes were removed and the supernatant was pipetted out of each. The pellets were washed with 1x DPBS to remove proteins from the penicillin/streptomycin and centrifuged again at 1264 rpm for five minutes. The supernatant was again pipetted out after centrifugation. The tubes were put on ice, and the cells in the pellet were suspended in 10 µL buffer Cytoplasmic Extraction Reagent I (CER1) (Thermoscientific 78833) and 5 µL protease inhibitor. The tubes were vortexed vigorously for 15 seconds then incubated on ice for 10 minutes. Ice-cold Cytoplasmic Extraction Reagent II (CERII) (5.5 µL) was then added, and the tubes were vortexed for another 5 seconds before going back on ice for one minute. They were taken off ice, vortexed once more for 5 seconds, then centrifuged at max speed for 5 minutes in the microcentrifuge.

The supernatant, containing the cytoplasmic extract, was transferred to pre-chilled tubes, labeled CE1, CE2, CE3, and CE4, and placed on ice to keep cold. The pellet remaining in the centrifuge tubes, which contained the cell nuclei, was suspended in 50 µL ice-cold Nuclear Extraction Reagent (NER) and 2.5 µL protease inhibitor. The centrifuge tube was vortexed at the highest setting for 15 seconds. The sample was put back on ice for 40 minutes, and vortexed for 15 seconds every 10 minutes. The tubes were then removed from ice and centrifuged at 16,000xg for 10 minutes. The supernatant, containing the nuclear extract, was transferred to a clean, pre-chilled tubes labeled NE1, NE2, NE3, and NE4, and put back on ice. Both the cytoplasmic extract and the nuclear extract were stored at –20°C.

**Protein Concentration/Quantification**

The cytoplasmic extracts and nuclear extracts from the T47D cells were analyzed and compared to standards to determine the protein concentration using a micro BCA protein assay kit (ThermoFisher Scientific 23235). A series of standards of varying concentrations were first prepared in 0.5 mL tubes using micropipettes. Using bovine serum albumin (BSA) at a concentration of 2 mg/mL and distilled water, the following array of protein concentrations were produced in eleven separate 0.5 mL tubes (note: tubes B through J use prior mixed tubes as their source of BSA).

Table 1. Micro BCA protein concentration standards prepared for protein concentrations assay using BSA at 2 mg/mL

| Tube | dd $H_2O$ added | BSA vol added | Final Concentration |
|---|---|---|---|
| **A** | 450 µL | 50 µL | 200 µg/mL |
| **B** | 400 µL | 100 µL from tube A | 40 µg/mL |
| **C** | 510 µL | 90 µL from tube A | 30 µg/mL |
| **D** | 250 µL | 250 µL from tube B | 20 µg/mL |
| **E** | 250 µL | 250 µL from tube C | 15 µg/mL |
| **F** | 250 µL | 250 µL from tube D | 10 µg/mL |
| **G** | 250 µL | 250 µL from tube E | 7.5 µg/mL |
| **H** | 250 µL | 250 µL from tube F | 5 µg/mL |
| **I** | 250 µL | 250 µL from tube H | 2.5 µg/mL |
| **J** | 250 µL | 250 µL from tube I | 1.25 µg/mL |
| **K** | 250 µL | 0 µL | 0 µg/mL |

Each of these volumes were added to the 0.5 mL tubes and mixed thoroughly but gently, and were stored at –20°C. The eight 2.1 µL protein extracts from the nuclear extracts and cytoplasmic extracts were each combined with 102.9 µL dd$H_2O$, creating a total volume of 105 µL. Each standard (100 µL ) was put into individual wells of a 96-well plate (Costar 2592), followed by NE1, NE2, NE3, NE4, CE1, CE2, CE3, CE4, and finally NER (nuclear extract reagent) and CER (cytoplasmic extract reagent), which were both added in duplicate. The 96-well plate thus contained the following, in columns 3-6:

Table 2. The 96-well plate layout for micro BCA protein concentrations assay with T47D breast cancer cell line

| | 3 | 4 | 5 | 6 |
|---|---|---|---|---|
| A | 0 µg/mL | 0 µg/mL | 30 µg/mL | 30 µg/mL |
| B | 1.25 µg/mL | 1.25 µg/mL | 40 µg/mL | 40 µg/mL |
| C | 2.5 µg/mL | 2.5 µg/mL | NER | CER |
| D | 5 µg/mL | 5 µg/mL | NER | CER |
| E | 7.5 µg/mL | 7.5 µg/mL | NE1 | CE1 |
| F | 10 µg/mL | 10 µg/mL | NE2 | CE2 |
| G | 15 µg/mL | 15 µg/mL | NE3 | CE3 |
| H | 20 µg/mL | 20 µg/mL | NE4 | CE4 |

Along with the 100 μL of protein-containing solution placed in the wells, 100 μL of a work solution was added to each well and mixed thoroughly with a pipette. The work solution contained 1750 μL micro BCA reagent A (MA) stock solution, 1610 μL reagent B (MB) stock solution, and 140 μL micro BCA reagent C (MC) stock solution. After sealing and a one hour incubation at 37°C, a SPECTRAFluor Plus was used to measure light absorbance of the plate to measure color change in the plate wells. Readouts were taken at 620 nm and 562 nm.

A second Micro BCA protein concentration assay was completed using the same methods for the standards, using the same BSA calculations as displayed in Table 1. A 96-well plate was filled using these standards and derivatives of a human prostate cancer cell PC-3 cells. Nuclear and cytoplasmic extracts along with NER and CER were again used in a 96-well plate. The CE derivatives were measure at 1:50 dilutions and in 1:100 dilutions. The experimental cytoplasmic and nuclear extract solutions were varied as well. The nuclear and cytoplasmic extracts 1 through 6 contained the following added solutions:

NE/CE1. Media control;
NE/CE2. 10 uM 1,10-phenanthroline;
NE/CE3. 30 uM PUGNAc;
NE/CE4. 10 uM MG132;
NE/CE5. 1,10-phen + PUGNAc; and
NE/CE6. MG132 + PUGNAc.

The plate was organized as follows:

Table 3. The 96-well plate layout for micro BCA protein concentrations assay with PC-3 prostate cancer cell line

| | 1 | 2 | 3 | 4 | 5 | 6 |
|---|---|---|---|---|---|---|
| A | 0 µg/mL | 0 µg/mL | 30 µg/mL | 30 µg/mL | CE1 (1:50) | CE4 (1:50) |
| B | 1.25 µg/mL | 1.25 µg/mL | 40 µg/mL | 40 µg/mL | CE2 (1:50) | CE5 (1:50) |
| C | 2.5 µg/mL | 2.5 µg/mL | NER (1:50) | CER (1:50) | CE3 (1:50) | CE6 (1:50) |
| D | 5 µg/mL | 5 µg/mL | NER (1:50) | CER (1:100) | CE1 (1:100) | CE4 (1:100) |
| E | 7.5 µg/mL | 7.5 µg/mL | NE1 (1:50) | NE4 (1:50) | CE2 (1:100) | CE5 (1:100) |
| F | 10 µg/mL | 10 µg/mL | NE2 (1:50) | NE5 (1:50) | CE3 (1:100) | CE6 (1:1000) |
| G | 15 µg/mL | 15 µg/mL | NE3 (1:50) | NE6 (1:50) | | |
| H | 20 µg/mL | 20 µg/mL | | | | |

Following the addition of the standards and the cellular extracts, which were added in quantity of 100 μL, a 100 μL volume of a work solution was added. This work solution was created using 0.1 mL C of the BCA reagents, 2.4 mL B of the BCA reagents, and 2.5 mL A of the BCA reagents. The work solution was mixed well into the wells and the plate was sealed and incubated for 1 hour at 37°C.

**Western Blot**

A buffer was created using 95 μL Laemmli sample buffer, which was added to a 1.5 mL tube along with 5 μL β-mercaptoethanol (βME) and mixed well. The NE1-4 and CE1-4 were removed from the freezer and thawed, then centrifuged. The volume necessary to get 15 μg of protein from each nuclear extract was calculated based on the protein concentrations found through the protein concentration assay and added to a clean 1.5 mL tube. The total volume was brought to 10.20 μL in each 1.5 mL tube using either NER (for NE tubes) and CER (for CE tubes). These solutions were mixed well with a pipette. The previously prepared buffer solution (10.2 μL) was added and again mixed well. Each of these 1.5 mL tubes were boiled in a hot water bath for about 5 minutes to denature the proteins then put on ice.

A second buffer was prepared for use in the western blot using 10x Tris/Tricine/SDS buffer solution (Bio-Rad 1610744). The 10x buffer solution (20 mL) was first mixed with 180 mL of $ddH_2O$ in order to dilute it to 1x. Blue ranger marker was loaded into the western blot gel well one in order to serve as the standard and to aid in estimating protein sizes. It was followed by NE1-4 in wells 2-5, LM cells were loaded into well 6, and CE1-4 was added into wells 7 to 10. The western blot was run at 40 mA constant current for 40 minutes, then at 100V for one hour. The reading from the western

blot was then transferred from the gel to a 0.45 μm nitrocellulose membrane in distilled water. Transfer buffer (5x, 200 mL) containing 3.03 g Tris base and 14.42 g of glycine was added to 100 mL methanol and 700 mL dd-$H_2O$ to dilute it to a 1x transfer buffer. The gel was soaked in this 1x transfer buffer, then ran through the transfer apparatus under water for 1 hour at 140 mA. Ice was placed outside the transfer apparatus to keep cold, and the transfer was completed on a stir plate with a bar. Ponceau S solution, negatively charged staining reagent which binds to the positive amino groups of the proteins, was used to stain the proteins on the membrane[17].

**Immunoprecipitation**

A Tris-buffered saline and Polysorbate 20 (or Tween 20) solution was made to aid in the blocking of proteins in order to prevent non-specific antibody binding during immunoprecipitation of the nuclear extracts. This Tris-buffered saline and Tween (TBST) solution contained 5 mL 1M Tris pH 6.8, 7.5 mL 5M NaCl, and 0.13 mL Tween 20 per 250 mL of solution. Protein rich milk was then prepared using 5 g dry blotting grade blocker milk (Bio-Rad 1706404) in 100 mL TBST. The membranes were blocked overnight at 4°C while coated in the 5% milk/TBST solution. The primary antibody used in immunoprecipitation for the HIF2α protein was an anti-HIF-2α polyclonal from Novus, which was diluted at 1 to 1000 in 5% milk/TBST (10μL antibody in 10 mL 5% milk/TBST). The primary antibody used for the HIF-1α protein was anti-HIF-1α monoclonal antibody at a concentration of 250 μg/mL, of which 1 μL was used. The antibodies were added to the plates and left for 1 hour at room temperature with rocking.

The plates were then washed once with 5% milk/TBST for 10 minutes with rocking, then a second and third time for 5 minutes each.

The secondary antibody, a goat anti-rabbit with horseradish peroxidase (HRP) (Pierce #1858415), was then added at a 1 to 3000 dilution. The plate was incubated at room temperature for 1 hour with rocking. The plate was then washed with TBST (without milk) for 10 minutes with rocking, then washed twice more with TBST alone for 5 minutes each with rocking. The membrane was left in TBST until it was ready to develop. Pierce enhanced chemiluminescence 2 (ECL2) western blotting substrate was used to aid in reactivity and detection. When it was ready to be used in western blotting, the excess TBST liquid was drained off and West Femto Maximum Sensitivity Substrate was put on membrane (1.5 mL of stable peroxide buffer and 1.5 mL of luminol enhancer solution). The membrane was soaked for 5 minutes then the excess liquid was drained.

**Western Blot for O-GlcNAC**

The proteins isolated from the immunoprecipitation were used in a second western blot, the procedure of which was the same as the earlier western blot. The first four lanes were filled with HIF-1α isolated proteins, and the second set of four lanes were filled with HIF-2α isolated proteins. The first lane of each set of four lanes contained the cells and media alone, the second lane of each set of four contained 10 μM 1,10-phenanthaline alongside the proteins, the third lane of each set of four contained 30 μM PUGNAc alongside the proteins, and the last lane of each set of four contained the proteins with both 10 μM 1,10-phenanthaline and 30 μM PUGNAc.

## Results/Discussion

The following tables were acquired from the SPECTRAFluor Plus as absorbance for the 96-well plate wells indicated in Table 2 and Table 3. The values are indicative of the light absorption measured at 562 nm.

Table 4. Light absorption in nm of micro BCA protein concentration assay with T47D breast cancer cell line (corresponding to Table 2)

| | 3 | 4 | 5 | 6 |
|---|---|---|---|---|
| A | 0.155 | 0.144 | 0.591 | 0.585 |
| B | 0.169 | 0.160 | 0.692 | 0.698 |
| C | 0.170 | 0.224 | 0.153 | 0.152 |
| D | 0.197 | 0.190 | 0.153 | 0.152 |
| E | 0.232 | 0.244 | 0.643 | 1.337 |
| F | 0.256 | 0.255 | 0.620 | 1.236 |
| G | 0.352 | 0.359 | 0.561 | 1.165 |
| H | 0.415 | 0.395 | 0.663 | 1.382 |

The protein concentrations of the cellular extracts were calculated using a line of best fit derived from the slope of the standards. The averages of the twice-added samples were calculated, and the following graph was created:

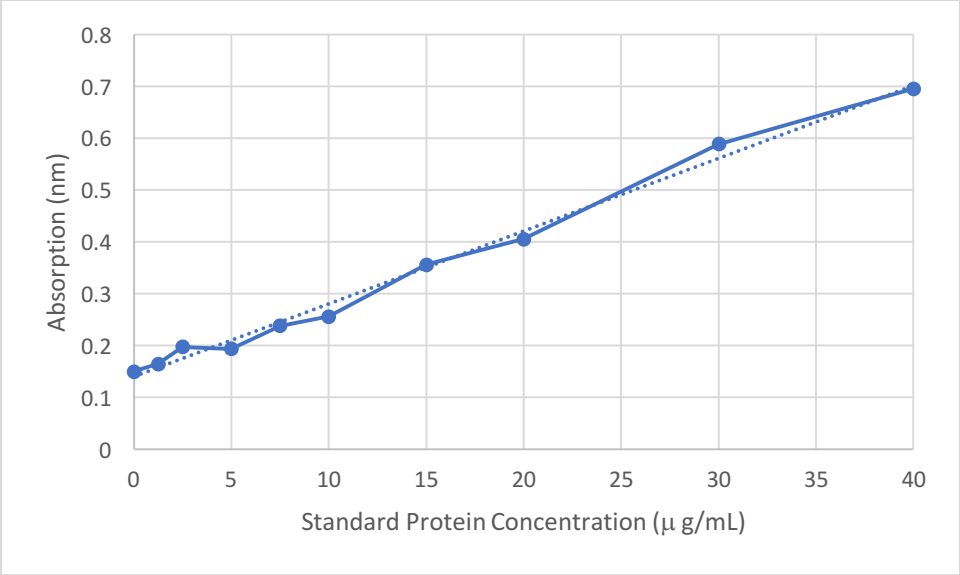


Figure 1. Graph of standard curve from micro BSA protein concentration assay with T47D breast cancer cells

The line of best fit had the formula

$$y = 0.0140x + 0.144$$

which was used to calculate the protein concentrations of the nuclear and cytoplasmic extracts from their absorption readings. These values were then multiplied by 50 for the 1 in 50 dilutions to arrive at the original protein concentration. The values for protein concentration of NE and CE were thus obtained.

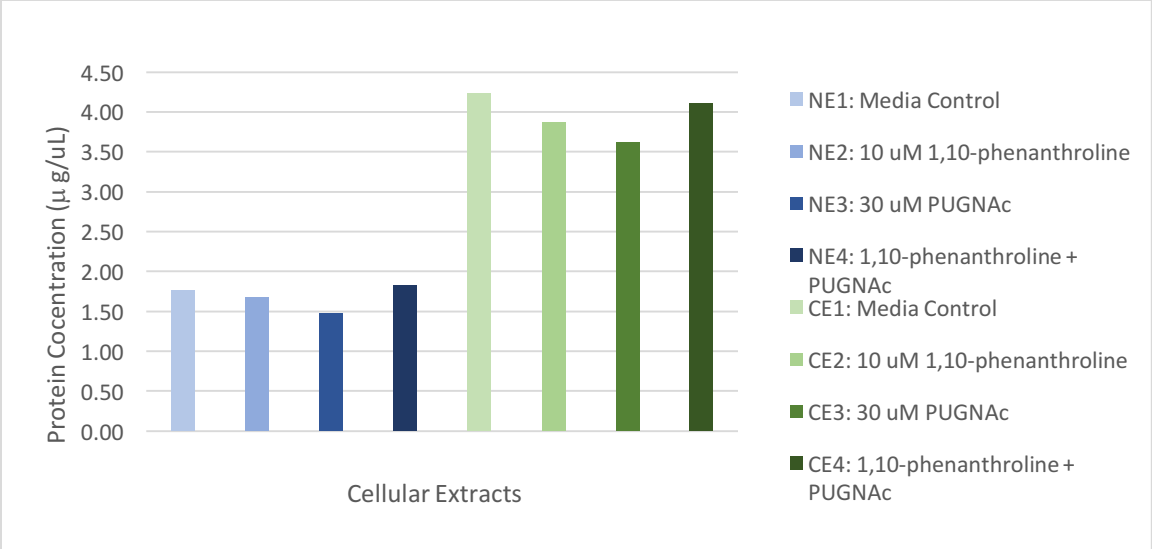


Figure 2. Protein concentrations of pre-diluted nuclear and cytoplasmic extracts of T47D cells

The cytoplasmic extracts contained a significantly higher concentration of proteins than the nuclear extracts. Both the nuclear extracts and cytoplasmic extracts displayed a slight decrease in protein concentration when exposed to 1,10-phenanthaline (10 µM); there was a 4.5% decrease in protein concentration in nuclear extracts and an 8.5% decrease in protein concentration in cytoplasmic extracts. However, there was a greater discrepancy between the control and the 30 µM PUGNAc exposed NE and CE. PUGNAc raises the levels of *O*-GlcNAc in the cells, which plays a role in the ubiquitination and subsequent degradation of proteins. Thus, in the case of the PUGNAc exposed NE and CE, a slight drop in protein concentration due to the heightened *O*-GlcNAc influenced protein degradation is appropriate. When combined with the 1,10-phenanthroline, which is used as a ligand, the *O*-GlcNAc binds to the proteins less often, causing a lack of a decrease in protein concentration.

Table 5. Light absorption in nm of micro BCA protein concentration assay with PC-3 prostate cancer cell line (corresponding to Table 3)

| | 1 | 2 | 3 | 4 | 5 | 6 |
|---|---|---|---|---|---|---|
| A | 0.113 | 0.115 | 0.574 | 0.583 | 1.044 | 0.986 |
| B | 0.138 | 0.142 | 0.716 | 0.721 | 0.988 | 0.868 |
| C | 0.162 | 0.157 | 0.123 | 0.130 | 0.988 | 0.869 |
| D | 0.188 | 0.190 | 0.123 | 0.115 | 0.662 | 0.619 |
| E | 0.227 | 0.222 | 0.574 | 0.556 | 0.649 | 0.561 |
| F | 0.276 | 0.273 | 0.580 | 0.598 | 0.640 | 0.545 |
| G | 0.328 | 0.345 | 0.605 | 0.571 | | |
| H | 0.448 | 0.424 | | | | |

The protein concentrations of the cellular extracts were again calculated using a line of best fit derived from the slope of the standards.

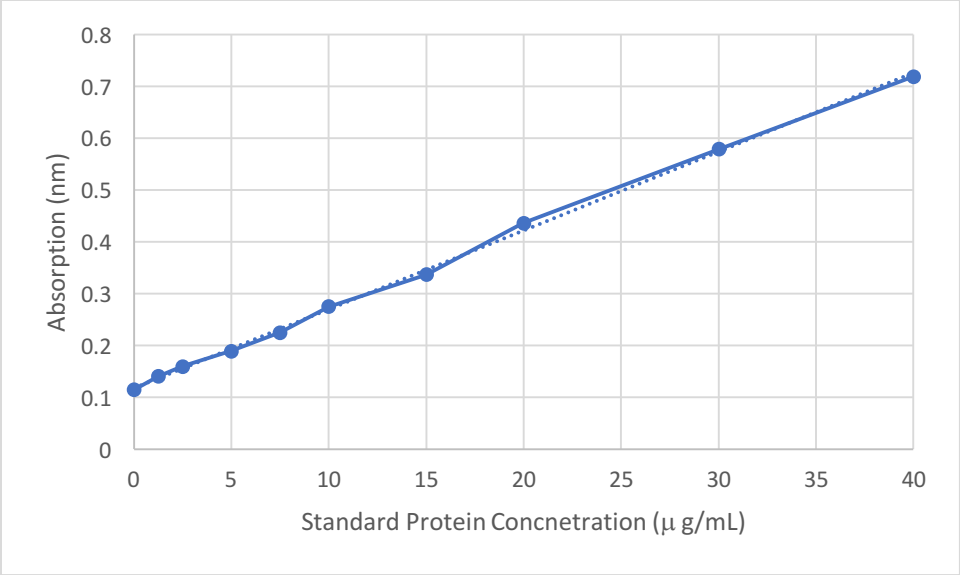


Figure 3. Graph of standard curve from micro BSA protein concentration assay with PC-3 prostate cancer cells

The line of best fit had the formula

$$y = 0.0152x + 0.115$$

which was used to calculate the protein concentrations of the nuclear and cytoplasmic extracts from their absorption readings. These values were then multiplied by 50 for the 1 in 50 dilutions and by 100 for the 1 in 1000 dilutions to arrive at the original protein concentration. The values for protein concentration of NE and CE were thus obtained.

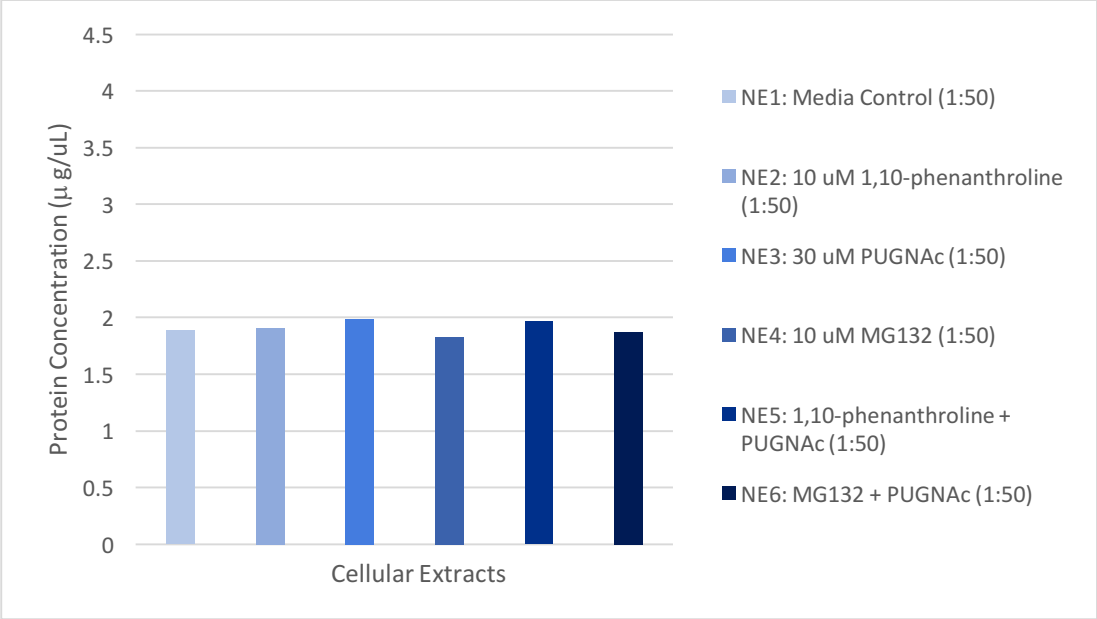


Figure 4. Pre-diluted protein concentrations of nuclear extracts of (1:50) PC-3 cells

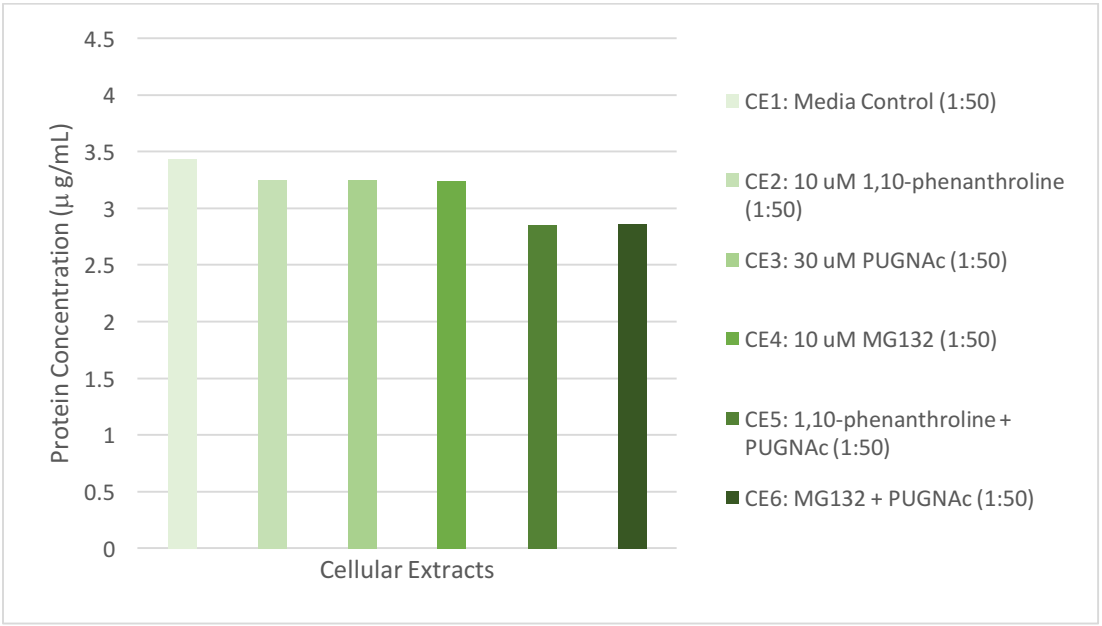


Figure 5. Pre-distilled protein concentrations of cytoplasmic extracts of (1:50) PC-3 cells

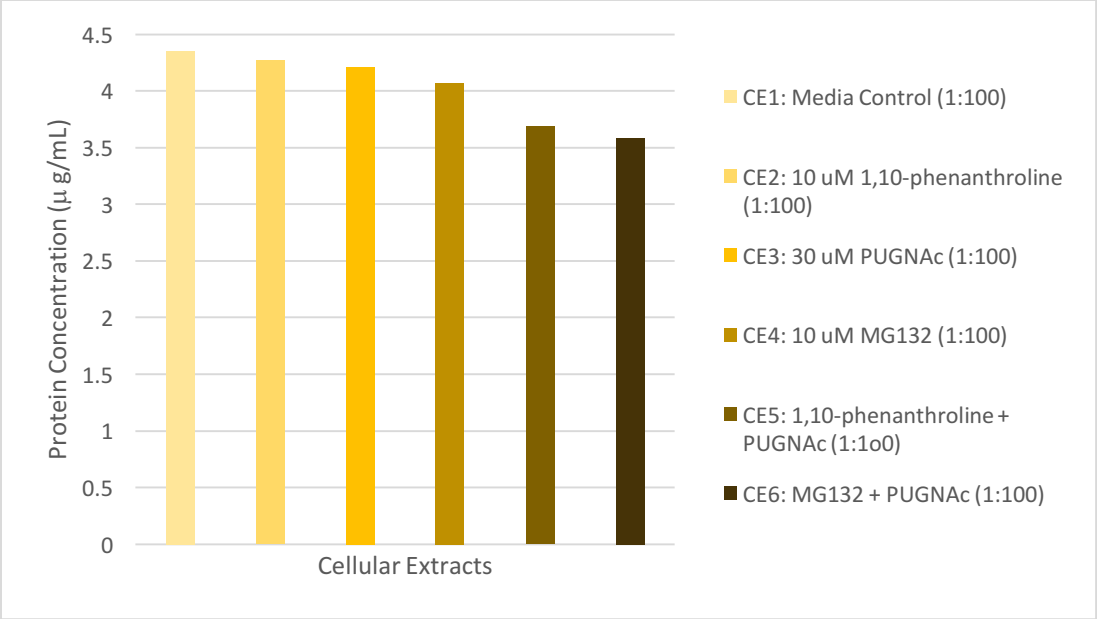


Figure 6. Pre-distilled protein concentrations of cytoplasmic extracts of (1:100) PC-3 cells

The inclusion of 10 µM MG132, a proteasome inhibitor, was expected to decrease the ubiquitination of proteins, especially when combined with 30 µM PUGNAc (which has been found to increase *O*-GlcNAc ubiquitination). This was expected to cause an overall increase in protein concentration. However, this was not displayed in either the nuclear extracts nor the cytoplasmic extracts. Instead, there was an overall drop in protein concentration exhibited for the cytoplasmic extracts, and the nuclear extracts saw no change in 10 µM MG132 added cells, even those including 30 µM PUGNAc. Furthermore, in the case of the nuclear extracts, the protein levels were notably similar to one another, with little deviation displayed between the control and the experimental cells. There was a much more significant differences in the cytoplasmic extracts, yet they often did not follow the expected trends of lower protein concentration in 30 µM

PUGNAc, nor did they follow the expected protein concentrations near the control for those with 10 μM 1,10 phenanthroline and 10 μM MG132.

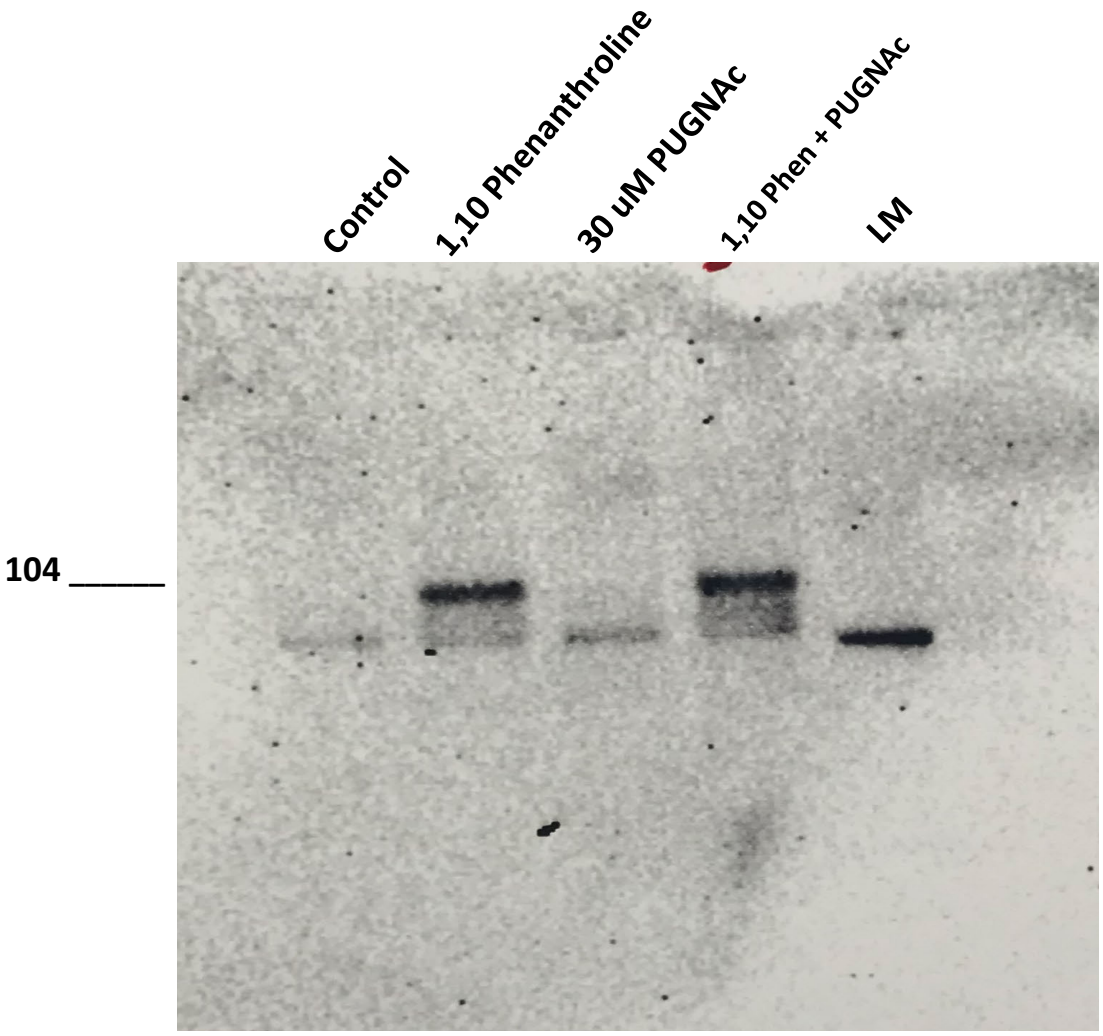


Figure 7. Western blot analysis of HIF-2α in nuclear and cytoplasmic extracts and LM cells

Blue ranger marker was loaded into the western blot gel well one, followed by NE1-4 in wells 2-5, LM cells were loaded into well 6, and CE1-4 was added into wells 7 to 10. Wells 7 through 10, containing the CE, did not produce any bands, indicating a lack of the protein. Furthermore, the nuclear extract wells including 1,10-phenanthroline

(wells 2 and 4) indicated the presence of HIF-2α proteins. The nuclear extract with 30 μM PUGNAc alone in well 3 displayed a lack of the HIF-2α protein. Since PUGNAc raises *O*-GlcNAc levels, and *O*-GlcNAc aids in protein degradation, it makes sense that the HIF-2α protein is not represented in this western blot. Furthermore, the expression of the HIF-2α protein in the lane with 1,10-phenanthroline and PUGNAc can be explained by the ability of 1,10-phenanthroline to form a ligand with *O*-GlcNAc and prevent the binding to and subsequent ubiquination of proteins, allowing them to be expressed in the western blot. This is evidence of the ability of *O*-GlcNAc to influence and interact with the HIF-2α proteins.


Figure 8. Western blot analysis of O-GlcNAc in nuclear extracts probed for HIF-1α and HIF-2α

The four left most wells contained HIF-1α proteins, with the first well containing a control media, the second containing 10 μM 1,10-phenanthroline, the third containing

30 μM PUGNAc, and the fourth containing both 30 μM PUGNAc and 10 μM 1,10-phenanthroline. The second set of four wells contained HIF-2α proteins, with the wells ordered from left to right containing the same experimental variables as the first four wells. Both the nuclear extracts and the cytoplasmic extracts display bands around the 104 kDa region for the PUGNAc containing wells, with a much stronger band present in the only PUGNAc containing well. This band is indicative of *O*-GlcNAc, the protein of interest. The presence of *O*-GlcNAc in those wells as opposed to those lacking PUGNAc is due to the upregulation of *O*-GlcNAc by PUGNAc. This shows that *O*-GlcNAc is able to bind to and interact with both of the HIF-1α and HIF-2α sets of proteins.

## Conclusions

The compound, *O*-linked β-*N*-acetylglucosamine, was found to influence the hypoxia-inducible factor proteins. These proteins are significant in the necessary alteration, continuation, and upregulation of cancer metabolism. *O*-GlcNAc plays a key role in changes in the metabolism of cancer cells and is thought to be a possible target for anticancer therapy. Though the results of this research are preliminary and far from complete, there is great promise in this area, and the results were significant in showing that *O*-GlcNAc is able to target the ever-relevant to cancer HIF-1α and HIF-2α proteins. The future of this research will look to discover the specific site of *O*-linked glycosylation and the mechanism by which this process occurs, along with the potential means one might have to interrupt such a process. Due to the impressive nature of cancer to not only survive but often thrive in low oxygen environments, thanks in part to HIF-1α and HIF-2α proteins, the disruption of such a mechanism could potentially shut down the pathways by which cancer is able to grow. The result could be the death or the cessation of growth of cancer cells, preventing metastasis and successfully halting the most potentially lethal aspect of the disease. However, these aspects of the research are beyond the scope of this experiment.

Bibliography


1. Balkwill, F. R., Capasso, M., & Hagemann, T. (2012). The tumor microenvironment at a glance. *Journal of Cell Science, 125*, 5591-5596. doi:10.1242/jcs.116392
2. Birner, P., Schindl, M., Obermair, A., Breitenecker, G., & Oberhuber, G. (2001). Expression of Hypoxia-inducible Factor 1 in Epithelial Ovarian Tumors: Its Impact on Prognosis and on Response to Chemotherapy. *Clinical Cancer Research, 7*, 1661-1668. Retrieved February 27, 2018, from http://clincancerres.aacrjournals.org/content/clincanres/7/6/1661.full.pdf
3. Bos, R., Hanrahan, C. F., Mommers, E. C., Semenza, G. L., Pinedo, H. M., Abeloff, M. D., . . . Wall, E. V. (2001). Levels of Hypoxia-Inducible Factor-1 During Breast Carcinogenesis. *Journal of the National Cancer Institute, 93*(4), 309-314. doi:https://doi.org/10.1093/jnci/93.4.309
4. DeBerardinis, R. J., & Chandel, N. S. (2016). Fundamentals of cancer metabolism. Science Advances, 2(5), e1600200. http://doi.org/10.1126/sciadv.1600200.
5. Hanahan, D., & Weinberg, R. A. (2011). Hallmarks of Cancer: The Next Generation. *Hallmarks of Cancer: The Next Generation, 144*(5), 646-674. doi: https://doi.org/10.1016/j.cell.2011.02.013
6. Hanahan, D., & Coussens, L. M. (2012). Accessories to the Crime: Functions of Cells Recruited to the Tumor Microenvironment. *Cancer Cell, 21*(3), 309-322. doi:https://doi.org/10.1016/j.ccr.2012.02.022
7. *Hart GW, Akimoto Y. The O-GlcNAc Modification. In: Varki A, Cummings RD, Esko JD, et al., editors. Essentials of Glycobiology. 2nd edition. Cold Spring Harbor (NY): Cold Spring Harbor Laboratory Press; 2009. Chapter 18. Available from: Https://www.ncbi.nlm.nih.gov/books/NBK1954/.*
8. Korneev, K. V., Atretkhany, L. N., Drutskaya, M. S., Grivennikov, S. I., Kuprash, D. V., & Nedospasov, S. A. (2017). TLR-signaling and proinflammatory cytokines as drivers of tumorigenesis Author links open overlay panel. *Cytokine, 89*, 127-135. doi:https://doi.org/10.1016/j.cyto.2016.01.021
9. Kosir, M. A., MD. (2018, January). Breast Cancer - Gynecology and Obstetrics. Retrieved February 19, 2018, from http://www.merckmanuals.com/professional/gynecology-and-obstetrics/breast-disorders/breast-cancer.
10. Kundu, J. K., & Surh, Y. (2008). Inflammation: Gearing the journey to cancer. *Mutation Research/Reviews in Mutation Research, 659*(1-2), 15-30. doi:https://doi.org/10.1016/j.mrrev.2008.03.002
11. Landskron, G., La, M. D., Fuente, Thuwajit, P., Thuwajit, C., & Hermoso, M. A. (2014). Chronic Inflammation and Cytokines in the Tumor

Microenvironment. *Journal of Immunology Research, 2014*. http://dx.doi.org/10.1155/2014/149185
12. Lu X, Kang Y. Hypoxia and hypoxia-inducible factors (HIFs): Master regulators of metastasis. Clinical cancer research : An official journal of the American Association for Cancer Research. 2010;16(24):5928-5935. doi:10.1158/1078-0432.CCR-10-1360.
13. Ma, Z. & Vosseller, K. Amino Acids (2013) 45: 719. https://doi.org/10.1007/s00726-013-1543-8.
14. Madell, R. (2017, June 13). Metastatic Breast Cancer: Life Expectancy and Prognosis (C. Chun MPH, Ed.). Retrieved February 19, 2018, from https://www.healthline.com/health/breast-cancer/metastatic-prognosis.
15. Nishida, N., Yano, H., Nishida, T., Kamura, T., & Kojiro, M. (2006). Angiogenesis in Cancer. Vascular Health and Risk Management, 2(3), 213–219.
16. Padua, D., & Massagué, J. (2008). Roles of TGFβ in metastasis. *Cell Research, 19*, 89-102. doi:doi:10.1038/cr.2008.316
17. Reinhart, M. P., & Malamud, D. (1982). Protein transfer from isoelectric focusing gels: The native blot. *Analytical Biochemistry, 123*(2), 229-235. Retrieved April 24, 2018, from https://www.sciencedirect.com/science/article/pii/0003269782904390?via=ihub.
18. Schito, L., & Semenza, G. L. (2016, December). Hypoxia-Inducible Factors: Master Regulators of Cancer Progression. CellPress, 2(12), 758-770.
19. Talks, K. L., Turley, H., Gatter, K. C., Maxwell, P. H., Pugh, C. W., Ratcliffe, P. J., & Harris, A. L. (2000). The Expression and Distribution of the Hypoxia-Inducible Factors HIF-1α and HIF-2α in Normal Human Tissues, Cancers, and Tumor-Associated Macrophages. The American Journal of Pathology, 157(2), 411–421.
20. Types of Breast Cancer. (2017, September 25). Retrieved February 20, 2018, from https://www.cancer.org/cancer/breast-cancer/understanding-a-breast-cancer-diagnosis/types-of-breast-cancer.html.
21. U.S. Breast Cancer Statistics. (2018, January 9). Retrieved February 20, 2018, from http://www.breastcancer.org/symptoms/understand_bc/statistics.
22. Vaupel, P., & Harrison, L. (2004, November 01). Peter Vaupel. Retrieved February 25, 2018, from http://theoncologist.alphamedpress.org/content/9/suppl_5/4.full.
23. Wang, M., Zhao, J., Zhang, L., Wei, F., Lian, Y., Wu, Y., … Guo, C. (2017). Role of tumor microenvironment in tumorigenesis. Journal of Cancer, 8(5), 761–773. http://doi.org/10.7150/jca.17648.
24. Zagzag, D., Zhong, H., Scalzitti, J. M., Laughner, E., Simons, J. W., & Semenza, G. L. (2000). Expression of hypoxia-inducible factor 1α in brain tumors.

*Cancer, 88*(11). doi:https://doi.org/10.1002/1097-0142(20000601)88:113.0.CO;2-W